Semi-automated Detection and Quantification of Aortic Atheromas from Three-Dimensional Transesophageal Echocardiography

Concetta Piazzese[1,3], Wendy Tsang[2], Miguel Sotaquira[1], Roberto M Lang[2], Enrico G Caiani[1]

[1] Politecnico di Milano, Dipartimento di Elettronica, Informazione e Bioingegneria, Milano, Italy
[2] University of Chicago, Chicago, USA
[3] USI, Universitá della Svizzera Italiana, Lugano, Switzerland

Abstract

Quantification of descending aorta atheromas (AT) with 2D transesophageal echocardiography (TEE) is time-consuming and underestimates plaque burden, while 3D TEE can provide the basis for analysis of AT 3D dimensions and volume. We developed a novel semi-automated algorithm to detect aortic AT in 3D TEE, to quantify their severity and volume and tested its accuracy compared to an expert gold standard. The 3D TEE datasets acquired from 58 consecutive patients were analyzed. Results showed a good accuracy in comparison with expert analysis, with an agreement of 95% in absolute presence/absence of AT per patient, 89% in AT number and location and 85% in patient risk due to AT severity classification. AT volumes were highly correlated (R^2=0.98), with a slight underestimation (9%) compared to manual measurements. The proposed semi-automated algorithm is rapid, feasible and accurate in analyzing AT from 3D TEE descending aorta datasets.

1. Introduction

Strokes are the fourth leading cause of death in the United States and transesophageal echocardiography (TEE) is routinely performed in stroke patients when an extra-cardiac source of embolism has not been identified [1]. Typically, at the end of the cardiac TEE examination the descending aorta is visualized while retracting the probe to identify complex atherosclerotic plaques. These atheromas (AT), considered complex if they are either > 4 mm in thickness, ulcerated or contain mobile thrombi, significantly increasing stroke risk [2,3]. However, two-dimensional (2D) TEE imaging allows the visualization and the measure of only one cross-sectional plane at a time, thus ignoring the three-dimensional (3D) morphology of the AT. This may result in underestimation of AT complexity and total burden.

We hypothesized that the recently available 3D TEE imaging technology applied to the aorta evaluation could provide the basis to quantify AT 3D dimensions and volume.

Accordingly, our aims were: 1) to develop a semi-automated software for detection and quantification of AT from 3D TEE images of descending aorta; 2) to assess its accuracy, compared to an expert gold standard, in the identification of the presence/absence of AT, their location and number, classification of AT associated severity risk, and computation of AT volume.

2. Methods

2.1. Study protocol

Clinically indicated TEE studies were performed in 58 consecutive patients (35 males, 60 + 16 years). 3D TEE (X-7t, Philips, Netherlands) datasets of the descending aorta were acquired, using single-beat, narrow-angle acquisition mode. These images were acquired at 0° with the TEE probe rotated towards the descending aorta. If no atherosclerotic plaque was present, a representative region of the descending aorta was imaged. If atherosclerotic plaque was present, non-overlapping 3D datasets were obtained from the level of the diaphragm to the aortic arch. These datasets were then exported in DICOM format for semi-automated analysis on a dedicated computer system.

2.2. Semi-automated atheroma analysis

An algorithm that requires minimal user interaction for AT segmentation and quantification was developed in C++ (VTK and ITK libraries).

3D Dataset Orientation. The first task re-orients the 3D volume such that one axis corresponds to the longitudinal dimension of the aorta. The orthogonal dimension of the

correct short-axis cut-plane of the aortic lumen is first obtained by navigating the 3D dataset and defining the volume of interest (VOI) through the selection of two slices that mark the ends of the aorta. Then, a point in each of these slices is selected, visually corresponding to the center of the aortic lumen. The line passing between these two points (i.e., the long-axis of the aorta) is computed and the 3D dataset is rigidly rotated.

True aortic lumen 3D mesh. After re-orientation, a 3Dmesh M of the true aortic luminal surface (including potential plaques along the wall) is generated by applying an automated thresholding to binarize the VOI and by using the marching cubes algorithm [4].

Ideal aortic lumen 3D surface. Assuming that the aortic lumen contour, in every short-axis cross-section, has an ellipsoidal 2D shape, five points on the aortic lumen wall, excluding the AT if present, are manually initialized to find the unique elliptical curve passing through them (Figure 1).

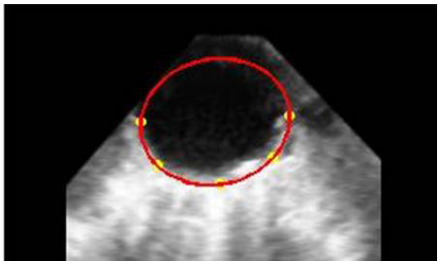

Figure 1. Five points initialization (in yellow) on a 2D short-axis cross-section to obtain the elliptical curve (in red) that represents the aortic lumen contour.

Starting from the canonical equation of the ellipse:

$$dx^2 + exy + fy^2 + gx + hy + l = 0 \quad (1)$$

the center (c_x,c_y), the major (a) and minor (b) axes, and the ellipse orientation (φ) are identified using the least squares minimization criterion. Then, the coordinates of the ellipse's points are calculated and the elliptical contour is generated:

$$x(t) = c_x + a\cos\vartheta\cdot\cos\varphi - b\sin\vartheta\cdot\sin\varphi \quad (2)$$

$$y(t) = c_y + a\cos\vartheta\cdot\sin\varphi + b\sin\vartheta\cdot\cos\varphi \quad (3)$$

This process is repeated on a total of seven equally-spaced short-axis planes in the VOI, from which the elliptical lumen contour in the planes in-between were obtained by linear interpolation (Figure 2). This luminal contour represents the ideal aortic lumen since aortic AT are excluded from the surface.

Segmentation: On each aortic 2D cross-sectional cut-plane in the VOI, the automated detection of the AT is performed by searching in the corresponding cut-plane of the mesh M the nodes (i.e., the vertices of the triangular patches constituting the mesh) that are inside the elliptical contour (Figure 3).

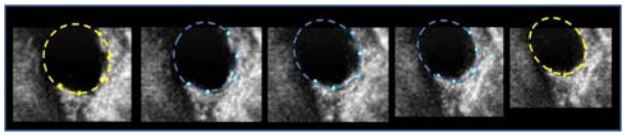

Figure 2. Yellow dashed line and points show the elliptical contours in two consecutive initialized short-axis planes corresponding to aortic cross-sections. For planes in-between, initialized points are linearly interpolated and thus the elliptical contour is calculated (in cyan).

Briefly, given m_i^n (x_i^n,y_i^n) the nodes of the mesh M in the *n-th* cut-plane, for each node the distance with the elliptical contour center (x_0^n, y_0^n) is computed as:

$$\rho\left(m_i^n\right) = \sqrt{\left(x_0^n - x_i^n\right)^2 + \left(y_0^n - y_i^n\right)^2} \quad (4)$$

together with its angular position θ_i^n in respect to a reference zero degree orientation (Figure 3).

Based on θ_i^n, the distance $r\left(\vartheta_i^n\right)$ between the corresponding point on the ideal aortic lumen elliptical contour and its center is computed as:

$$r\left(\vartheta_i^n\right) = \frac{a^n \cdot b^n}{\sqrt{\left(b^n \cdot \cos\left(\vartheta_i^n\right)\right)^2 + \left(a^n \cdot \sin\left(\vartheta_i^n\right)\right)^2}} \quad (5)$$

where a^n and b^n are the major and minor axes lengths of the *n-th* ellipse. Finally, $\rho\left(m_i^n\right)$ and $r\left(\vartheta_i^n\right)$ are compared:

- if $\rho\left(m_i^n\right) < r\left(\vartheta_i^n\right)$, the node m_i^n is classified as a potential AT node and the difference $r\left(\vartheta_i^n\right)$ - $\rho\left(m_i^n\right)$ represents the local thickness;
- if $\rho\left(m_i^n\right) \geq r\left(\vartheta_i^n\right)$, the node m_i^n is classified as a non-AT node.

Once this process has been repeated for all cut-planes in the VOI, the number of nodes composing each potential AT is counted, and only AT characterized by more than 300 nodes (set empirically to avoid multiple small plaques due to possible noise in the mesh) are retained.

AT severity associated risk grading and volume computation. Finally, the 3D mesh is visualized, with the detected AT highlighted using a 3-level color map (green, mild risk: between 1-2 mm; yellow, moderate risk: between 2-4 mm; red, high risk: > 4 mm) based on their local thickness (Figure 4B). For each AT, the maximum thickness determines the semi-automatic AT associated severity risk grade. Moreover, for each AT, its internal volume was computed using the method of disks.

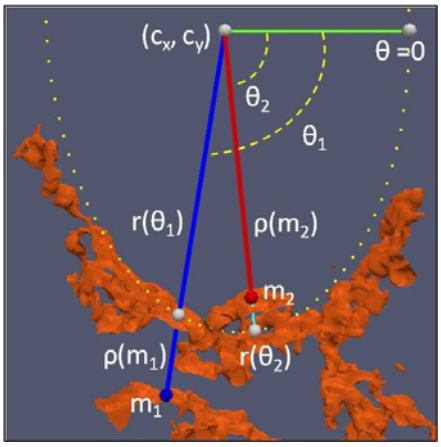

Figure 3. Schematization of the automated atheroma segmentation for the nodes associated to the 2D *n-th* cross-sectional cut-plane of the mesh M. For nodes m_1 and m_2: their distances ($\rho(m_1)$ and $\rho(m_2)$) to the elliptical lumen center (c_x, c_y) are compared with the corresponding distances $r(\theta_1)$ and $r(\theta_2)$ of the points (in white) on the ideal ellipse contour. In this example, the node m_1 will be classified as non-atheroma, while the node m_2 will be classified as a potential atheroma node.

2.3. Gold standard analysis

An experienced cardiologist, blinded to the results of the semi-automated detection, used multi-planar analysis of the 3D TEE datasets (QLAB 9.1, Philips, USA) to determine the gold standard (GS) results.

Plaque detection. AT were visually identified in a systematic cranial to caudal direction using three orthogonal views. For each AT, a screenshot of the rendered 3D volume (Figure 4A) and the cross-sectional cut planes that intersected the AT were exported. A second independent observer then compared the semi-automated program output (Figure 4B) to the rendered 3D volume screenshot for assessing the correctly detected AT in number and location.

Plaque risk severity grading. For each AT, the thickest dimension was manually measured on a 2D cut-plane perpendicular to the base of the AT, and used for grading the associated severity risk as mild, moderate or high using the same scale as the semi-automated program.

Plaque volume computation. To test the accuracy of the semi-automated software in quantifying the AT volume, fifteen datasets containing isolated AT were selected, and manually traced with custom software to derive AT boundaries in cross-sectional slices. The AT volume was then calculated using the method of disks.

2.4. Statistical analysis

Agreement and Kappa values were calculated to determine software accuracy against the GS with respect to: 1) the presence or absence or AT per patient; 2) the number of AT per patient; 3) AT associated severity risk. Kappa analysis was performed with linear weights. Automated and manual measurements of AT volumes were compared by linear regression and Bland-Altman analyses.

3. Results

Analysis of the 3D datasets was possible in all patients requiring on average 5 minutes each, including data retrieval, pre-processing and initialization. Manual analysis varied from 5 to 30 minutes, depending on number and complexity of plaques.

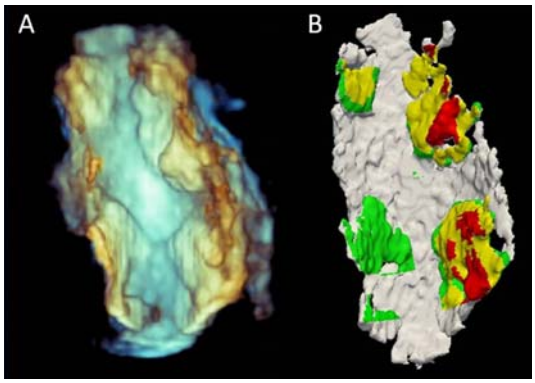

Figure 4. Example of comparison between the 3D rendered TEE data (A) and the 3D segmented mesh of the aortic lumen (B), visualized with the detected atheromas highlighted using a 3-level colormap based on their local thickness, related to their associated risk (green, mild: between 1-2 mm; yellow, moderate: between 2-4 mm; red, high: > 4 mm).

The semi-automated detection agreed with the GS in presence or absence of AT in 55 patients and disagreed in 3 patients. Location and number of AT were semi-automatically identified correctly in 145 out of 162 AT. Thus, on a per patient basis, agreement with respect to the number of AT was 89% with a kappa value of 0.89.

In terms of associated severity risk, overall, in 116 of the 145 semi-automatically identified AT, there was no difference with the GS (80% agreement, kappa value 0.64). When considering the maximum AT severity risk per patient, the agreement between the GS and the software increased to 85% (kappa value 0.78). Of the remaining 29 AT, no one differed by more than one grade in severity risk from the GS (by the algorithm, 15 had a decrease in severity by 1 grade and 14 had an increase in severity by 1 grade).

The Bland-Altman (Figure 5A) analysis showed that semi-automatic segmentation underestimated (9%)

volumes with respect to manual segmentation. The limits of agreement (0.78 and 1.02) indicate a possible underestimation (22%) or overestimation (2%) error. Also, a high correlation (R^2=0.98, p<0.001) between semi-automated and manual measurements was found (Figure 5B).

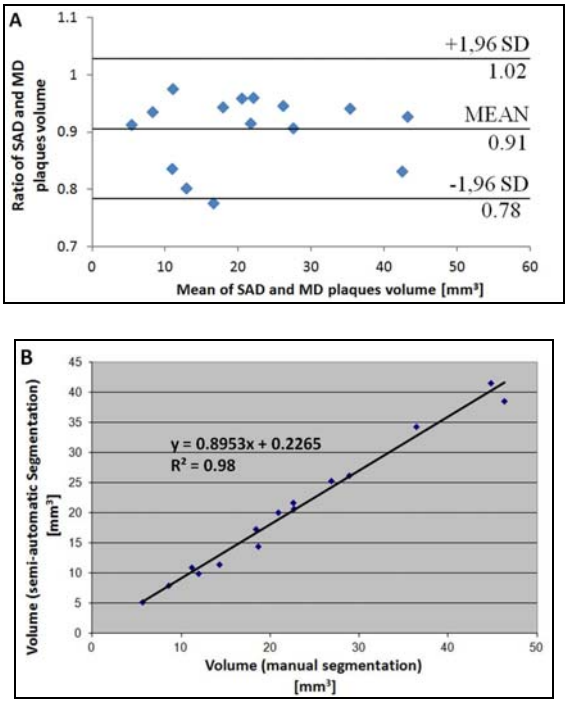

Figure 5. (A) Bland-Altman analysis between the semi-automatically detected (SAD) and manually detected (MD) atheroma volume (B) Linear correlation between the manually and semi-automatically detected atheroma volume.

4. Discussion

This study demonstrates that semi-automated detection and quantification of atheromatous plaques in 3D TEE datasets of the descending aorta is rapid, feasible and accurate for AT presence, severity and volume.

3D TEE allows visualization of the entire AT morphology and the assessment of its complexity. However, without dedicated software, AT identification and analysis from 3D TEE datasets results in a tedious and time-consuming manual procedure.

To the best of our knowledge the proposed semi-automated algorithm represents the first approach in which AT quantification is provided, thus giving the clinician 3D AT information in a rapid and accurate manner, with minimal user interaction.

The choice to describe the 2D aortic lumen as an elliptical contour proved adequate allowing to accurately describe the profile even in presence of partial dropout of the aortic wall.

The high accuracy in AT detection and associated severity risk grading demonstrates the feasibility of the proposed approach in clinical practice. In this setting, the 3D parametric display of the results could guide the visual inspection of the 3D TEE data, thus reducing the time of analysis. The quantification of AT volume could lead to new criteria to classify AT severity, taking into account the entire 3D plaque morphology, rather than the undimensional measurement of thickness.

The fact that the analysis was limited to the proximal descending aorta represents a limitation; since the accuracy of the algorithm in the ascending aorta and aortic arch was not tested. Also, AT calcium content, affecting videointensity, was not considered in the current analysis.

5. Conclusions

We developed a semi-automated method for the detection and quantification of descending aortic atheromas from 3D-TEE datasets. This analysis is rapid, feasible and accurate in determining atheroma number, severity, and volume. This methodology allows standardization of 3D atheroma quantification, with great potential benefits in clinical practice.

References

[1] Hoyert DL, Xu J. Deaths. Preliminary Data for 2011. National Vital Statistics Reports. October 10, 2012 2012;61(6):1-64.

[2] Tunick PA, Rosenzweig BP, Katz ES, Freedberg RS, Perez JL, Kronzon I. High risk for vascular events in patients with protruding aortic atheromas: a prospective study. J Am Coll Cardiol 1994;23:1085-1090.

[3] Kronzon I, Tunick PA. Aortic atherosclerotic disease and stroke. Circulation 2006;114:63-75.

[4] Lorensen WE, Cline HE. Marching cubes: A high resolution 3D surface construction algorithm. ACM SIGGRAPH Computer Graphics. July 1987 1987;21(4):163-169.

Address for correspondence:
Dr Enrico Caiani
Dipartimento di Elettronica, Informazione e Bioingegneria
Politecnico di Milano, Piazza L. da Vinci 32, Milano, Italy
enrico.caiani@polimi.it